

# INTEGRATED STRUCTURAL HEALTH MONITORING AND ENERGY HARVESTING POTENTIAL OF BUILDING

SOGARWAL AKASH M. SINGH

M.Tech Student, Department of Civil Engineering (Structure), MGM'S Jawaharlal Nehru Engineering College, Aurangabad.

V.T. MORE

Assistant Professor, Department of Civil Engineering, MGM'S Jawaharlal Nehru Engineering College, Aurangabad.

**Abstract-** Piezoelectric materials have so far proven their efficacy for both energy harvesting and structural health monitoring (SHM) individually. Piezoelectric ceramic (PZT) patches, operating in d31-mode, are considered best for SHM. However, for energy harvesting, built up configurations such as stack actuators are more preferred. The main objective of this research was to explore the possibility of employing the same piezo sensor for SHM as well as energy harvesting on real-life civil structures such as bridges. Experiments have been carried out in the laboratory environment to measure the voltage and the power generated by PZT patches in surface bonded as well as embedded configurations. In embedded form, the PZT patches have been considered in the form of concrete vibration sensor (CVS), operating in the normal axial strain mode. Beam structure has been considered for modelling as well as lab experimentation owing to the energy harvesting potential offered by real-life Structure. Utilization of the same patch for energy harvesting as well as for SHM through a combination of the global vibration and the local EMI techniques has been experimentally demonstrated. Proof-of-concept demonstration of normal plate type piezo in axial strain mode in place of commercial expensive transducers for energy harvesting from real-life civil structure has been the original aspect of this study. It is expected that the outcomes of this research will pave way for dual use of the ordinary piezo patch in SHM as well as energy harvesting. With recent advancement of Internet of Things (IoT) and client-side web technologies, wireless integrated sensor devices nowadays can process real-time raw sensor signal data into target measurements, such as displacement, and then send the results through a standard protocol to the servers on the Internet (i.e., the cloud). The monitoring results are further processed for visualization purpose in the servers and the computed results are pushed to connected clients like browsers or mobile applications in real-time.

**Keywords:** SHM, piezometer, beam, piezo patch.

## 1. INTRODUCTION

### 1.1 BACKGROUND

Everything around us is getting smarter and changing. The change is taking step toward a better and smart future. The major role of engineering focus to play a pivotal role in bringing those changes to make a point-breaking understanding of the technologies around us in a better way. A smart home can make a smart city, likewise a smart industry can revolutionize the process for a smarter maintenance. It is a small step in making smart industries by reducing the complexity of wired communication with replaceable—connecting devices and cloud platform for analysis and control. This also solves the problem of complex hardware architecture by replacing structural complexity with logical devices and advanced communication devices. This paper aims to deploy computing techniques in creating a barrier to integration, complexity, to provide more financial gains and energy savings. Sustainability of resources in many small- and medium-scale industries is a current dominant issue. Automated process is a very efficient and effective process on installing very-high-configured equipment, which is a possible constraint in small and medium industries. Consistent growth in market defines targets, but lack of resources has become a possible challenge in many ways. A simple consideration of a mushroom harvesting plant, where the production process takes minimum of 14 weeks for the yield and most of the approach, is manual. A conveyor system would possibly reduce time of transporting yield; maintain the same environment and easy handling. But yet most of the process is manual and all the information is recorded by a person. This has a possible disadvantage of failure in certain conditions. The problem persists in many other companies, where the process is dependent on manpower. To avoid problems of human error and to utilize all the manpower for a better production, this paper provides a brief insight of possible advantages of IoT in automation industry. Initiating the process, identifying metal from nonmetal, handling the part as per requirement are the general insights briefed in this paper with real-time deployment. Usage of IoT concepts helps to monitor the process from any part of the world. One needs not to possibly be live at the moment to see the process. All the processes can be recorded, sorted, and are ready for analytics at an instance.

Structural health monitoring (SHM) is currently attracting huge research funding across the world. Experts have identified SHM as one of the top ten technologies having the potential of driving the global economy HM, especially for large civil structures, needs a mega network of sensors distributed throughout the structure. Powering these sensors is a critical issue. It either requires a distributed network of wiring or warrants installation of individual batteries, both of which call for huge investment. Fortunately, the power requirement of the sensors generally is low, ranging from micro to milli watts, and reducing further day by day. This has catalyzed research efforts to explore the possibility of employing renewable energy sources to power the sensors. The use of piezoelectric materials to act as generators for converting the vibrational energy of structures into electrical energy is one such possibility being explored rigorously over the last three decades. Piezoelectric ceramic (PZT) patches, operating in d31-mode, are considered best for SHM. However, for energy harvesting, built up configurations such as stack actuators are somewhat more preferred. The main objective of this thesis is to explore the potential of employing the same piezo sensor, operating in d31-mode, for SHM as well as energy harvesting on real-life structures.

### 1.2 MOTIVATION

All structures are subjected to slow and continued deterioration, caused by several factors, such as environmental degradation, fatigue, excessive loads, vehicle impacts and prolonged extensive usage. Even a minor incipient damage carries the potential to

grow out of proportion, culminating in collapse, thereby leading to disruption of services and/or loss of life and property. External loads due to construction, occupancy, vehicle movement, blast/ impact, and the associated stresses and deflections along with structural response, if monitored for occurrence of damages, the process is called as structural health monitoring (SHM).

### 1.3 CAUSES OF DETERIORATION OF STRUCTURES:

A structure becomes deteriorated for the following reasons

#### Site Selection and Site Development Errors:

Failures often result from unwise land use or site selection decisions. Certain sites are more vulnerable to failure. The most obvious examples are sites located in regions of significant seismic activity, in coastal regions, or in flood plains. Other sites pose problems related to specific soil conditions such as expansive soils or permafrost in cold regions.

#### Design Errors:

These failures include errors in concept that lack of structural redundancy, failure to consider a load or combination of loads, deficient connection details, calculation errors, misuse of computer software, detailing problems including selection of incompatible materials, failure to consider maintenance requirements and durability, inadequate or inconsistent specifications for materials or expected quality of work and unclear communication of design intent.

#### Construction Errors:

Such errors may involve excavation and equipment accidents; improper sequencing; inadequate temporary support; excessive construction loads; premature removal of shoring or formwork; and non-conformance to design intent.

#### Material Deficiencies:

While it is true that most problems with materials are the result of human errors involving a lack of understanding about materials, there are failures that can be attributed to unexpected inconsistencies in materials.

#### Operational Errors:

Failures can occur after occupancy of a facility as the result of owner/operator errors. These may include alterations made to the structure, change in use, negligent overloading and inadequate maintenance.

### 1.4 PROBLEM STATEMENT

Piezoelectric materials have so far proven their efficacy for both energy harvesting and structural health monitoring (SHM) individually. Piezoelectric ceramic (PZT) patches, operating in d31-mode, are considered best for SHM. However, for energy harvesting, built up configurations such as stack actuators are more preferred. The main objective of this research was to explore the possibility of employing the same piezo sensor for SHM as well as energy harvesting on real-life civil structures such as bridges.

### 1.5 SCOPE OF PROJECT

So far, the piezo sensors have been independently employed for SHM and energy harvesting. Keeping in view the background given above, it is justified to pursue the present study to develop a conceptual framework which can integrate the two functions using same PZT patch. The main objective of this thesis is to investigate the potential of utilizing the same PZT patch for SHM as well as energy harvesting employing axial strain actuation (d31) mode

### 1.6 OBJECTIVE

- 1- To developing and validating analytical suitable for computation of harvestable energy from the piezo patches operating in d31-mode, either in surface bonded or embedded configurations, including
- 2- The effect of losses such as the mechanical loss, the dielectric loss and the shear lag loss and to extend the analytical model to real-life structures.
- 3- To performing detailed parametric studies to work out the optimum size and parameters of the patches from energy harvesting considerations.
- 4- To Use of normal plate type piezo in axial strain mode in place of commercial expensive transducers for energy harvesting has been the innovative aspect of this study.

## 1. LITERATURE REVIEW

**Brinda Chanv et al. [1]** presented Structural Health Monitoring stands out as the appearing field in civil engineering which provides the possibility for continuous and regular assessment of the security and integrity of civil infrastructures. It includes method of determining and detecting damages and weaknesses in the infrastructure because of aging or almost any other reason, good in time therefore a preventive maintenance is usually performed before it collapses. It is able to also provide warning about present state of the framework. Internet of little things (IoT), is the system of smart sensors that combine sensing and wireless transmission of important security parameters of buildings and components, to distant computing devices of which continually perform the processing and monitoring of these variables. This particular paper surveys the state of the existing exploration in the solutions plus implementation methods and tries to perform a comparative analysis.

**Debajyoti Misra et al. [2]** In this paper, we've suggested a smart creating health monitoring system to stay away from undesirable mishaps. Some accidents take site without any warning. The job within this newspaper provides an internet of little things (IoT) based building health monitoring (BHM) program. The program comprises piezoelectric sensors, ESP8266 Wi-Fi module and Arduino. Piezoelectric sensor (PZT) is used to produce and also get Lamb waves and also the received wave is even further examined to identify the health of the concrete structure. The strategy is different and utilizes cloud and mobile app based monitoring. You will find two essential features of the suggested system; it monitors the destruction in concrete construction and uploads the information on the cloud server. The extraordinary method takes the help of cloud sever method because of its positive location of data usability, ease of access as well as disaster recuperation. This proposed system generates all details related to structural health of a certain building and will inform on the responsible authority for remedial measures. So that it is able to avoid mishaps and save properties, money, and lives.

**Yang et al. [3]** presented this paper for the finite element simulation of the interaction between a PZT patch and a host structure, including the bonding layer, utilizing the EMI technique with varying temperature. He performed the simulation of the PZT–structure interaction at the high frequency range (up to 1000 kHz) using FEM software, ANSYS version 8.1.

**Duan et al. [4]** reviewed the implementation of piezoelectric transducers in health monitoring. The analysis of plain piezoelectric sensors and actuators and interdigital transducer and their applications in beam, plate and pipe structures for damage detection are reviewed in detail.

**Yang et al. [5]** implemented Piezo-electric ceramic Lead Zirconate Titanate (PZT) based EMI technique for SHM to various engineering systems. In this paper he used the structural mechanical impedance extracted from the PZT electromechanical conductance signature as the damage indicator. A comparison study on the sensitivity of the electromechanical admittance and the structural mechanical impedance to the damages in a concrete structure is conducted. Results show that the structural mechanical impedance is more sensitive to the damage than the electromechanical admittance thus a better indicator for damage detection.

**Zhang et al. [6]** studied the EMI technique for health monitoring. In this paper, he presented an impedance model for predicting the electromechanical impedance of a cracked beam. He analysed a coupled system of a cracked Timoshenko beam with a pair of PZT patches surface bonded to the top and bottom of the beam. He introduced the shear lag model to describe the load transfer between the piezoelectric patches and the cracked beam. He simulated the beam crack as a massless torsional spring.

**Yang et al. [7]** applied Piezo-electric transducers, working on the EMI technique for health monitoring in aerospace, civil and mechanical engineering. The piezoelectric transducers are usually bonded on the surface of the structure and subjected to excitation so as to interrogate the structure at the desired frequency range. The interrogation resulted in the conductance signatures which can be used to estimate the structural health or integrity according to the changes of the signatures.

**Chhabra et al. [8]** dealt with the Active Vibration control of structures with piezoelectric patches bonded on top and bottom surfaces of the beam. The patches are located at the different positions to determine the better control effect. The study is demonstrated through simulation in MATLAB.

**Peng [9]** studied the mechanical properties of steel fiber reinforced concrete crack for SHM. Since working environment is very harsh, the steel fiber reinforced concrete is prone to crack and a small crack on beam may result in severe damage. Hence, it is important to examine the mechanical properties of steel fiber reinforced concrete crack to detect early crack semiotics. He inspected the mechanical characteristics of steel fiber reinforced concrete crack by experimental tests on four specimens. He considered the effect of the loading position in the tests.

**Hong et al. [10]** modelled a strain-based load identification for beam structures subjected to multiple loads. In his model, he measured the contribution of each load to the strains by strain sensors. In this paper, the longitudinal strains measured from multiplexed fiber Bragg grating (FBG) strain sensors are utilized in the load identification.

**Parameswaran et al. [11]** studied the response of the mechanical systems from undesirable vibrations during their operations. Their occurrence is uncontrollable as it depends on various factors. However, for efficient operation of the system, these vibrations have to be controlled within the specified limits. Light weight, rapid and multi-mode control of the vibrating structure is possible by the use of piezoelectric sensors and actuators and feedback control algorithms. In this paper, direct output feedback based active vibration control has been implemented on a cantilever beam using Lead Zirconate-Titanate (PZT) sensors and actuators. Three PZT patches were used, one as the sensor, one as the exciter providing the forced vibrations and the third acting as the actuator that provides an equal but opposite phase vibration/force signal to that of sensed so as to damp out the vibrations. The designed algorithm is implemented on Lab VIEW 2010 on Windows 7 Platform.

**Hu et al. [12]** studied the application of Piezo-electric lead zirconate titanate (PZT) as a new smart material for health monitoring. To study the damage detection properties of PZT on concrete slabs, simply supported RCC slabs with PZT patches surface bonded to the host structure were chosen as the objective of the research and the electromechanical impedance technique was adopted for research. Five different kinds of damage were analysed to test the impedance values at different frequency bands.

**Neel Mania et al. [13]** studied The smart phones nowadays equip themselves with in-built sensors, such as Samsung Note 4 with heartbeat sensors including gyro meter and accelerometer incorporated in smart phones signals with remote servers, which can accelerate medical services in spatial-temporal dimensions. The latency reduction is one of the necessary features of computing platforms which can enable completing the healthcare operations, especially in large-size medical projects and in relation to providing sensitive and intensive services.

**Segun O et al. [14]** studied To address the scarceness of energy, wireless energy transfer (WET) techniques that exploit radio frequency (RF) signal to transfer RF energy has recently emerged for powering IoTSNs. This line of research is referred to as wireless power sensor networks (WPSNs). Consequently, an EE optimization problem is formulated for the successive WPSN system and solved by exploiting the problem structure and through a meta-heuristic algorithm. The new system is validated through the numerical simulation results presented in this work by thoroughly analysing, evaluating and comparing the proposed meta-heuristic based WPSN system with the baseline state-of-the-art WPSN systems that combined a meta-heuristic algorithm, two additional meta-heuristic algorithms including genetic algorithm (GA) and ant-colony optimization (ACO) algorithm as well as a non-meta-heuristic algorithm – specifically an iterative based Dinkelbach algorithm

**Oliver Mörth et al. [15]** studied Realizing performance improvements requires actual and relevant information about the current production provided to the management. However, the huge amount of data hinders a fast and correct decision making of the production manager as the extraction of the relevant information still appears to be a major problem the basis for the required decisions builds the proper providing of relevant information. IoT application are considered as one solution for realizing an efficient and effective monitoring a concept for IoT based monitoring of environmental conditions in the production area. Fulfilling the defined constraints scalability, adaptability and cost-effectiveness, a corresponding demonstrator has been developed and implemented in the LEAD Factory

### 3. METHODOLOGY

#### 3.1 Working Principle

Arduino Uno: Intelligent devices play a very crucial role in embedded systems. Most common MCU device by ATMEL is being used in Arduino Uno [12]. Being an open-source platform, it is preferably used in various projects on electronics and embedded systems. A physical circuit with MCU will be driven by the software program through IDE that runs from computer to the board (Fig. 5). ESP8266. Esp8266 is an open-source IoT platform. It includes firmware which runs on Wi-Fi (Fig. 6). A command from

user will initiate the process; the part on the conveyor system is identified by a metal sensor integrated over the system. An ultrasonic sensor will identify the exact position of the part over conveyor and stop the sequence; every piece of working can be monitored by a custom-designed Webpage 1tuch.in. Programming Steps for Programming Arduino Uno Board

1. Connect Arduino Uno to USB port of computer.
2. Initialize the board by selecting type of board being used and also with virtual port assigned to the board in the tools menu. Real-Time System Monitoring and Control of Automation Industry ... 1095.
3. An Arduino Uno sketch usually has five parts: declaring the variables; enabling the setup routine, which will initialize the variables and conditions to run the preliminary code; looping, is the place you add the main algorithm which will be executed repeatedly till an external reset is actively pressed or the sequence is terminated by the user; final section will be for other important functions to activate during the setup enablement and for loop routines.
4. To test the device, upload a preloaded program. This will ensure the device functioning.
5. Once after testing, the board is ready for any purpose deployment. Once disconnecting from computer and integrating it with proposed projects directly.

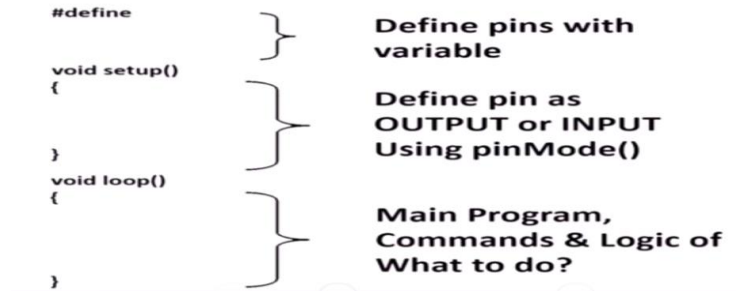


Fig. Program Structure in ARDUINO UNO

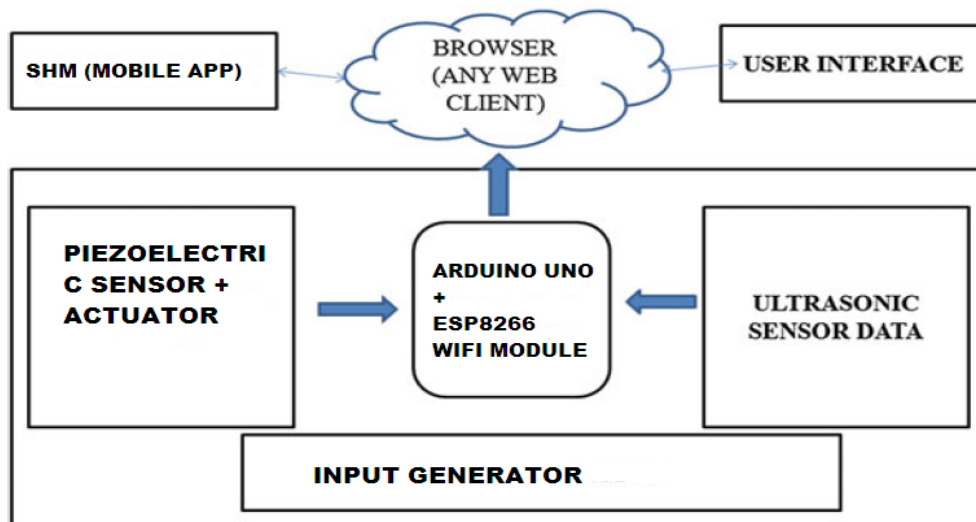


Fig. IOT Based SHM System Using ARDUINO UNO Program

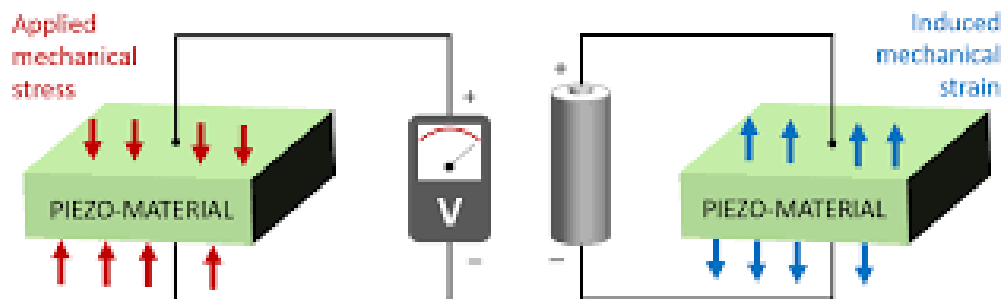


Fig. Coupling Effect of PZT Materials Used For SHM



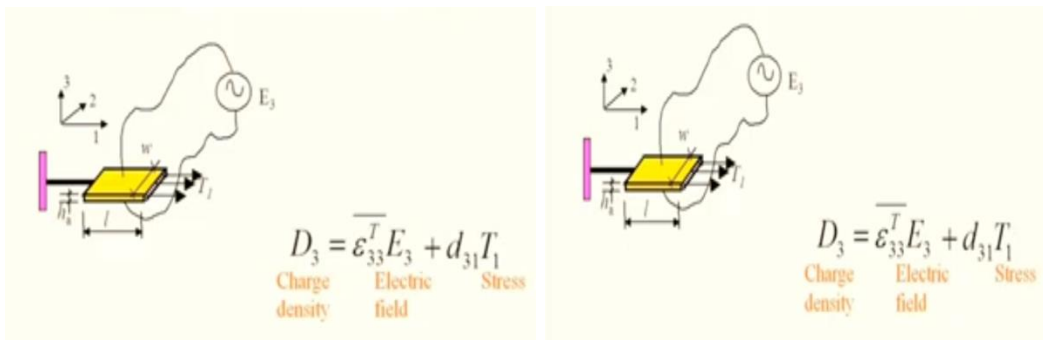


Fig. Constitutive Relation of PZT

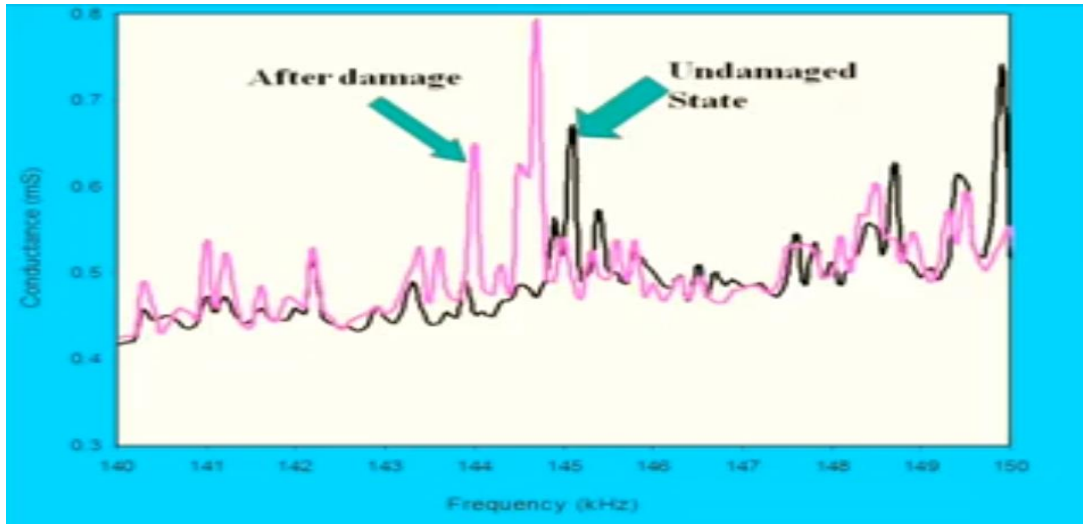


Fig. Signature Graph Showing Relation between Structural and Electrical Parameter Based on EMI Coupling

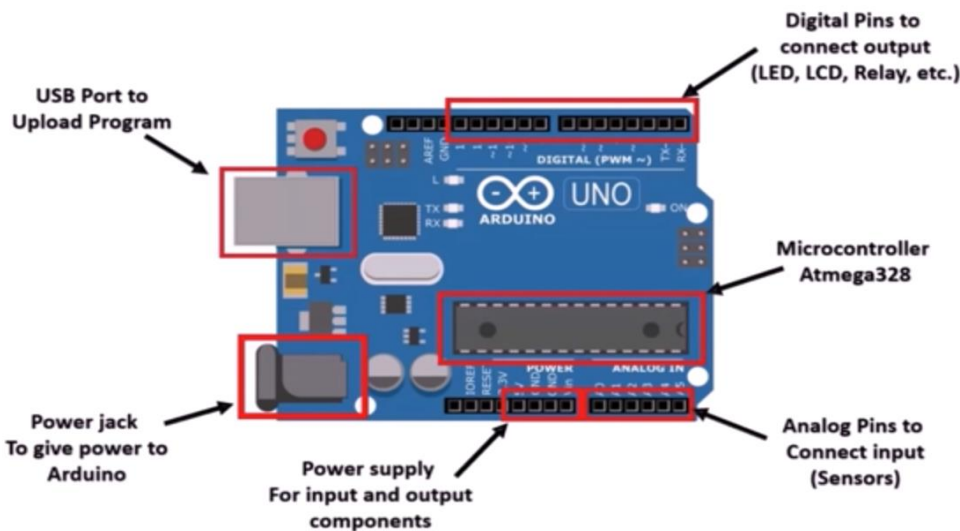


Fig. Microchip Physical Model of ARDUINO UNO

### 3.2 Finite Element Modeling

Finite element modeling of the mechanical part is very similar to what was discussed in the previously except that the coupling Terms introduce additional energy terms in the vibrational statements which results in additional coupling matrices in the FE formulation. Introduction of Piezoelectric material introduces an additional degree of freedom in the FE formulation. This additional DOF can be the electrical potential (Normally referred to as which is related to the Electrical field vector=  $E + E, 1 + E =$  ) or electrical field itself. Alternatively, the analysis can be performed by using conventional beam, or plane stress element derived earlier and the effects of coupling terms can be translated as equivalent concentrated nodal loads such an approach is possible when we assume that the sensing and actuation law are not coupled which is mostly true in piezoelectric material We will demonstrate both approaches.

This problem can be statically reduced to a problem of a cantilever beam with an end moment  $M$  shown, The moment  $M$  needs to be determined from the constitutive law of the PVDF material. The beam under 1-D state of stress with the stress acting in the  $x$  direction.

From Equ (a). we have

$$\{\sigma\} = [S]^{-1} \{\mathcal{E}\} - [S]^{-1} [d] \{E\}$$

The inverse of the compliance matrix is the constitutive matrix [C] and representing  $[e] = [S]^{-1} [d]$  the above equation becomes  $\{\sigma\} = [C] \{\mathcal{E}\} - [e] \{E_z\}$ .

The first part of the above equation is due to mechanical load, which is zero in the present case and hence is not relevant to the present problem. Since the beam is in 1-D state of stress, only  $\sigma_{xx}$ , bending stress in the axial direction, exists.

• The only material property of relevance here is the Young's Modulus Y and the relevant piezoelectric coefficient is  $e_{31}$ , which is first elements of third row of the matrix [e] given in the above Equation. Hence the constitutional law can be written as

$$\sigma_{xx} = -e_{31}E_z = -e_{31}V/t.$$

From the elementary beam theory, we have

$$M/I = \sigma_{xx}/Z$$

where M the moment acting on the cross section, I is the moment of Inertia of the cross section, and Z is the coordinate in the thickness direction.

Substituting for from Eqn. above in the elementary beam equation, we can express the moment developed due to electrical excitation is given by

$$M = 2e_{31}VI/t^2$$

From the theory of deflection of beams, we can show that the transverse displacement  $w(x)$  of a cantilever beam with a tip moment  $M$  is given by,

$$W(x) = -Mx^2/2EI$$

Using the value of Moment M, we can write the displacement variation is a bimorph piezoelectric cantilever beam as

$$w(x) = (e_{31}Vx^2/Et^2) \text{ and } w(L)_{elec} = (e_{31}VL^2/Et^2) \dots \dots \dots @ x=L$$

Next, in addition to electric field, we will introduce mechanical load P applied at the tip.

Deflection of a cantilever beam bested to tip concentrated load P is  $w(x) = P/EI * (x^3/6 - x^2L/2)$

The tip deflection in this case is got by substituting  $x=L$  in the above equation, which is equal to

$$w(L)_{mech} = -PL^3/3EI$$

Now, when both mechanical and electrical loads are applied, the total deflection will be sum of the deflections due to mechanical load and electrical load. which given by

$$w(L)_{total} = -PL^3/3EI + e_{31}VL/et$$

From this expression, we see that as the voltage is increased, it reduces the net downward deflection due to the mechanical load. The above expression can also give the voltage necessary to force the total deflection equal to zero, which is given by

$$V = PL/e_{31}bt$$

It is clear that the presence of electrical load helps to totally eliminate the deflection of the cantilever beam due to mechanical load. This in essence, is the main principle of actuation, which can be exploited for a variety of applications such as vibration control, noise control or shape controlled structures.

### 3.3 Experimental Setup for Cyclic Loading Test

In this particular work, 2 non ductile RC frame specimens which are retrofitted by adding a shear wall (RCW2 and RCW1) are evaluated under cyclic loading. A non-ductile RC frame was built then and first rebar connections have been post installed and also wall structure rebar cage had been installed, as depicted in Figure one. Concrete was at last cast to develop an RC shear wall structure, as offered in Figure two. Figure three shows the sizes as well as wall structure panel reinforcements of RCW and RCW1 two; the thickness of the wall board is fifteen cm. In order to enhance ductility, the reinforcements in the wall sections of equally RCW2 and RCW1 are placed to forty five degrees from horizontal. The reinforcements in the wall sections are placed identically in each specimen. These two specimens are the boundary columns with a cross sectional area of  $30 \times 50 \text{ cm}^2$ . Each column is fashioned with primary bars of 8-D19 and 4-d22 & a transverse reinforcement of D10/20cm in both ends. The net reinforcement of the shear wall is attached to the current RC frame using adhesive rebar's. The inserted length of the adhesive reinforcement is twelve cm along with the lap length of the reinforcements is thirty cm. Figure four displays the plan of reinforcements of the boundary columns as well as beams. Table one presents the yielding energy as well as supreme power of the reinforcement in the examples. Table two presents the hostile concrete strengths in the wall board, foundation and boundary column.



**Figure 3.1**RC frame and the reinforcement arrangement of the post-installed wall of RCW1  
**Table1.**Yield and ultimate strengths of there in for cements of the specimens (unit:MPa).

#4 (D13)		#6 (D19)		#7 (D22)	
Yielding	Ultimate	Yielding	Ultimate	Yielding	Ultimate
371	550	365	371	365	550



**Figure3.2.** The front view of the specimen RCW1.

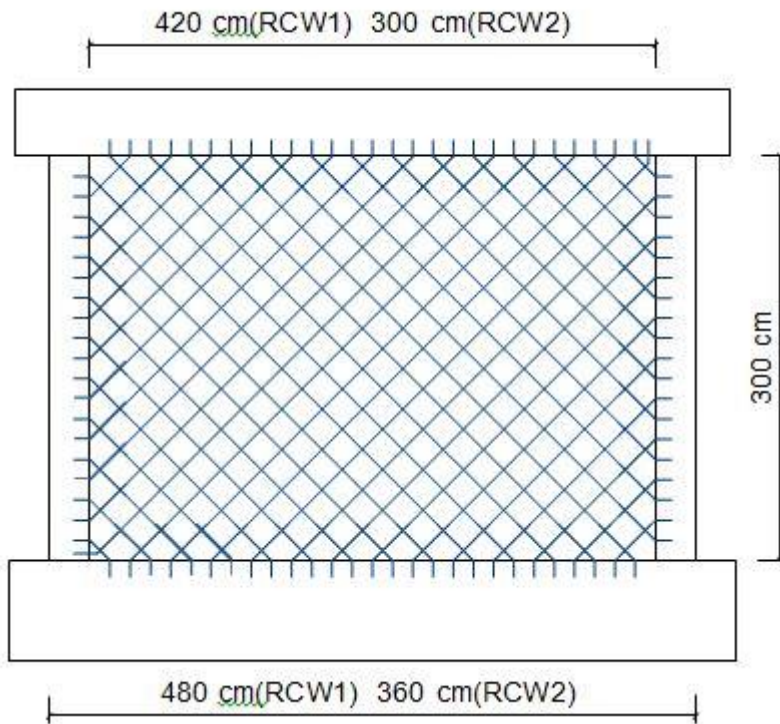


**Figure 3.3**Dimensions of the specimens of RCW1 and RCW2. (unit: cm).



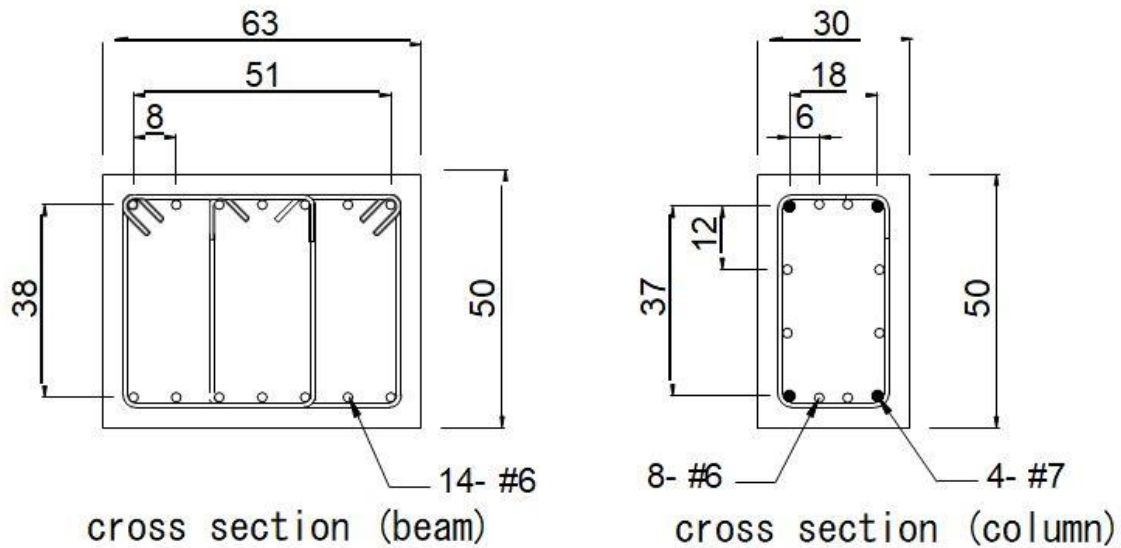


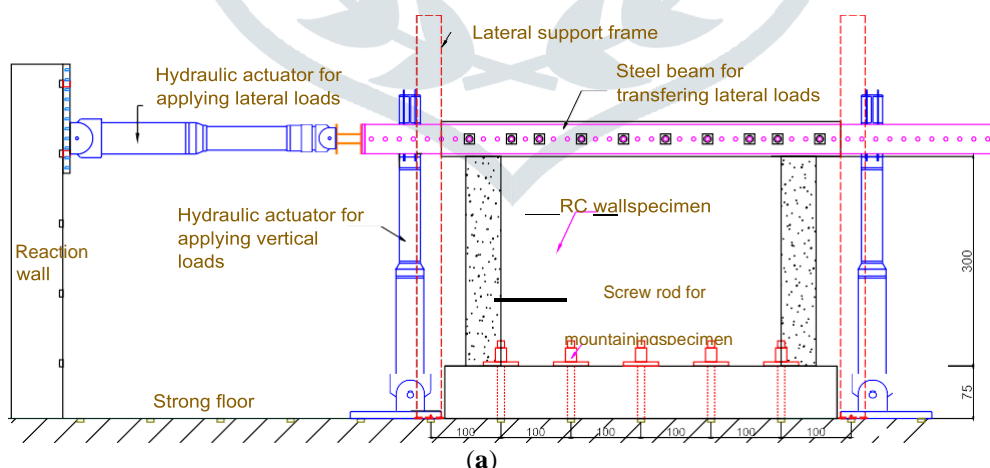
Figure 3.4 Dimensions and reinforcements of the column and beam (unit: cm).

Table 2 Concrete compressive strength of the specimens (unit: MPa).

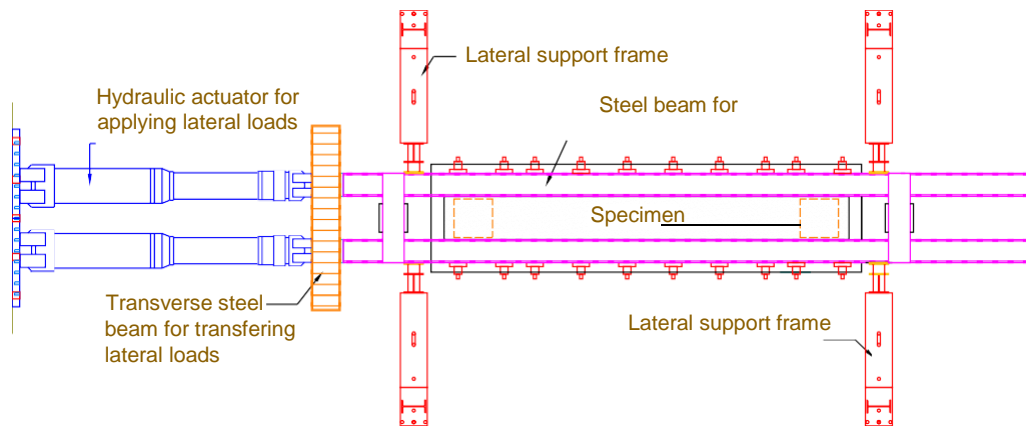
Specimen	Foundation	Frame	RC Panel
RCW1	11.6	13.7	25.9
RCW2	24.3	19.6	21.8

The loading system in this particular effort contains actuators, lateral support frames along with a steel rigid beam of loading distribution as shown in Figure five. The loading technique incorporates vertical and horizontal actuators to use vertical and horizontal loading on the tested specimen. Horizontal loading simulates seismic force. Vertical loading simulates a gravitational load. It was put on to ninety for vertical of each column making use of the 2 vertical hydraulic actuators equipped on the 2 sides of the wall structure sample throughout the evaluation. According to the loading distribution steel rigid beam as well as steel anchor bolts, vertical and horizontal loadings might be assumed to get uniformly sent out into the beam of the sample.

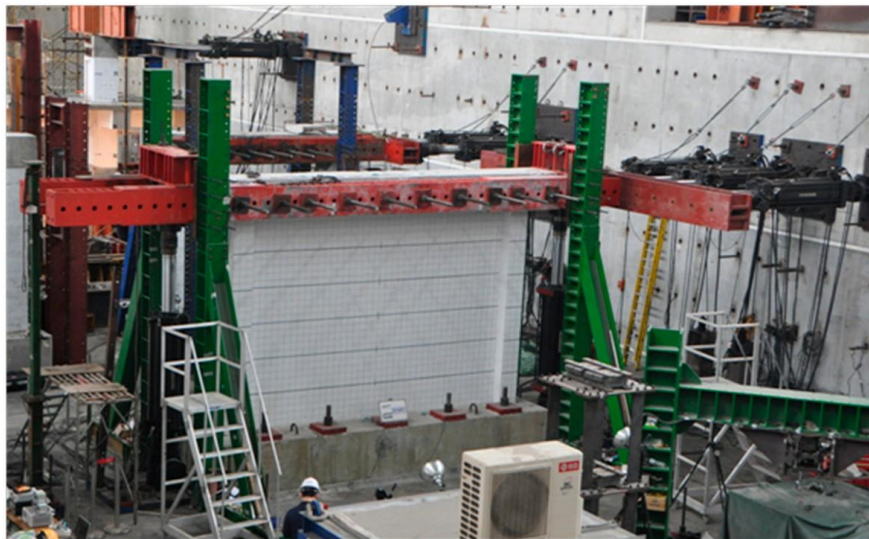
The load cell on the beam end was used to calculate the horizontal a lot which were used by the actuators. Linear deviation displacement transducers (LVDT) have been utilized to calculate the best as well as bottom horizontal displacements of the wall panel along with a dial gauge was accustomed keep track of the deformation of the base. Figure five shows a configuration drawing in addition to photograph of the arrangement for the reversed cyclic loading test. Steel bracing frames have been placed on each side of the examined specimen to avoid unforeseen torsional activity of the wall structure specimen. A reversed cyclic loading test was carried through with a predetermined increment of drift ratio in each action until the sample fully failed







(b)



(c)

**Figure 3.5** Experimental set-up of the cyclic loading test, (a) lateral view, (b) top view and (c) the photo

The loading system in this particular work contains the actuators and also a rigid beam of loading distribution, as shown in Figure five. The put on loading system in this particular work has the vertical and horizontal actuators and also might use the vertical and horizontal loading on the specimen, individually. The horizontal loading might be utilized to simulate the seismic force. The vertical loading might be utilized to simulate the gravity load applied into specimens. It was applied ninety for vertical of each column making use of the 2 vertical hydraulic actuators equipped on the 2 sides of the wall structure sample throughout the evaluation. Bottom on the loading division steel beam as well as steel anchor bolts, the vertical and horizontal loading might be assumed uniformly disperse into the beam of specimens. The load cell equipped on the beam end was used-to calculate the horizontal lots used by the actuators. The linear variation displacement transducers (LVDT) have been utilized to calculate the best as well as bottom horizontal displacements of the wall board as well as the control gauge was accustomed keep track of the groundwork deformation. The setup design in addition to picture of the test established for the reversed cyclic loading test is revealed in Figure five. Steel bracing frames have been placed on the 2 sides of the examined specimen to stay away from the sudden torsional activity of the wall structure specimen. Reversed cyclic loading evaluation was carried out by using a predetermined raising drift ratio for every action up until the total failure of the sample.

#### 4. RESULT AND DISCUSSION

The structural health monitoring evaluation is dependent on the usage of several PPTs as actuators to produce propagation emphasize waves as well as others as sensors to get the waves. The amplitude of propagation waves is attenuated by the presence of damage and cracks within the concrete wall building, leading to the transmitted energy of the propagation waves to drop as the amplitude decreases of theirs. This particular effort put on the cyclic horizontal lots on the best beam of the examples working with the displacement management, as shown in Figure eight. For the sample of RCW1 in the drift ratio of 0.25 %, the small cracks created horizontally at the bottom end of the boundary columns. Furthermore, the fractures with a tendency angle close to forty five degrees dispersed uniformly in the area of the wall board. At the drift ratio of 0.5 %, the break advancement is similar to the drift of 0.25 %. Nevertheless, bottom end and the foundation of the boundary columns have small spalling of concrete coverage since the compressive strength of theirs of concrete is comparatively smaller compared to the wall board. Figure 4.2 displays the cracking patterns in every drift amount and also the last disaster condition of the sample in the drift ratio of 1.0 % and also the concrete in the bottom end of the boundary columns as well as foundation crushed in the next cycle. The experimental results exhibited that the basis of the current RC frame is significantly weaker than the retrofitted RC wall. Next, the failure might be located in the user interface of the basis of the current RC frame as well as the retrofitted RC wall. The chief cracks could be located on the positions of the basis of the current RC frame underneath the boundary columns. Because of the specimen was

damaged in bending conduct, the center part of the user interface of the basis of the current RC frame as well as the retrofitted RC wall structure wasn't discovered with way too many cracks

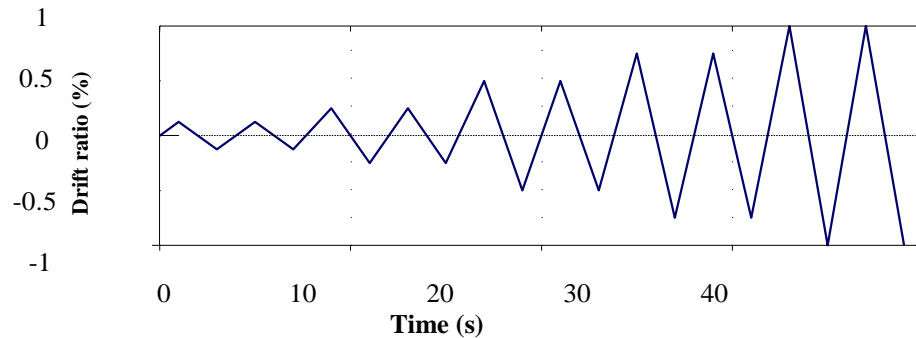
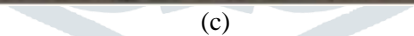
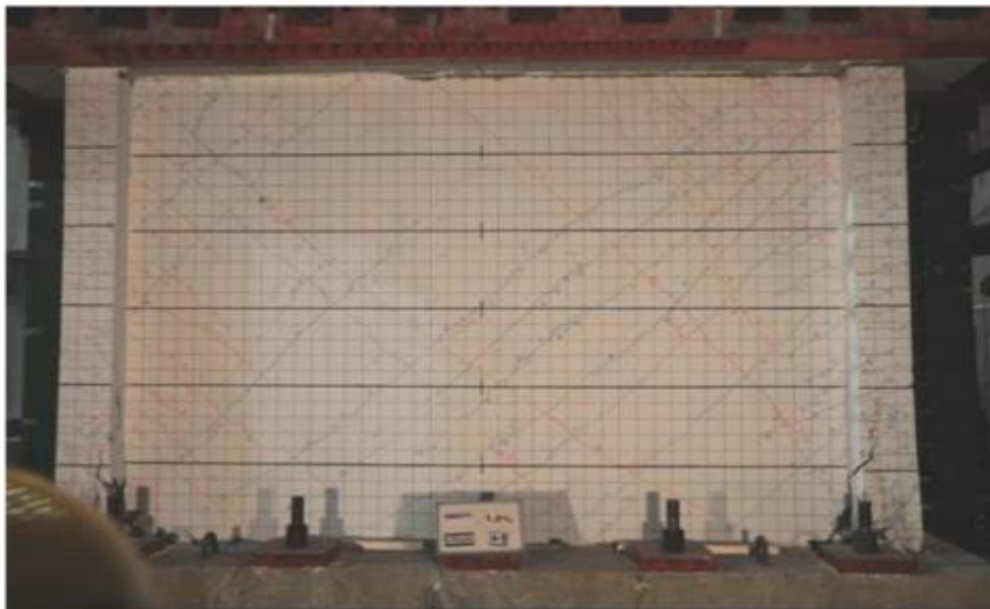
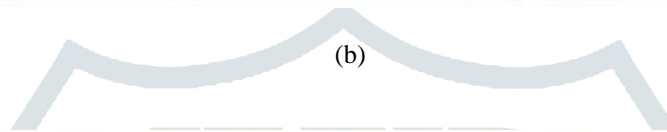
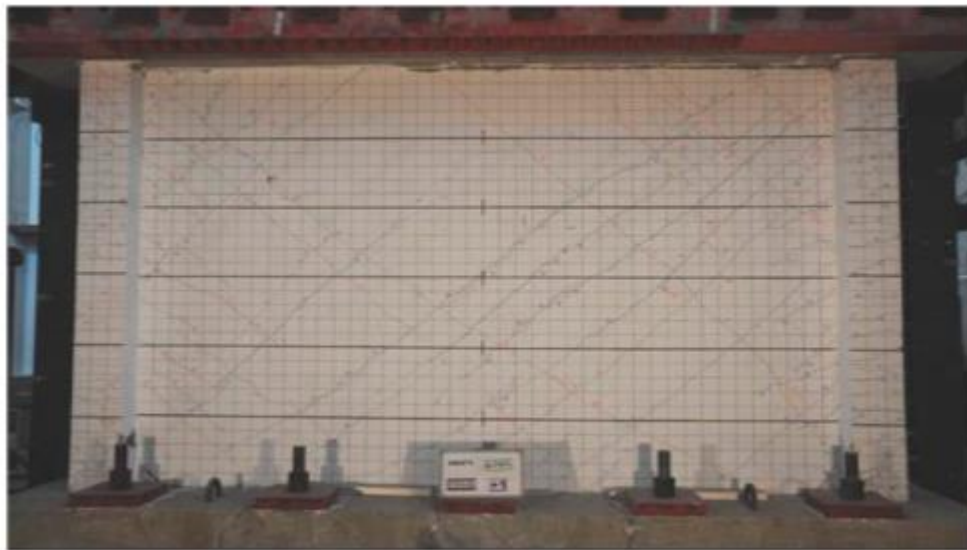


Figure 4.1. Loading history of the reversed cyclic loading test.

For the sample of RCW2 in the drift ratio of 0.25 %, the crack advancement is similar with RCW1. Whenever the drift ratio reached 0.5 %, the lengthy fractures together with the width of one mm in the user interface in between the RC wall board as well as best beam are found. Figure 4.3 displays the cracking patterns in every drift amount and also the last failure condition of the specimen. The failure setting of RCW2 happens in the drift ratio of 1.0 % where the concrete at the high end of the boundary columns and also in the wall structure premier nook crushed in the next cycle. This particular experimental results demonstrated that the strength of the user interface of current RC frame as well as the retrofitted RC wall structure isn't strong adequate to transport the shear pressure. Next, the disappointment might be located in the user interface of the beam of the current RC frame as well as the retrofitted RC wall. The disappointment of the user interface of the wall and the beam had also been causing the failure of boundary columns. Piezoelectric-based sensing was utilized to do the SHM of the tested RC wall structure after particular drift throughout the test. The energy based injury index, provided by Equation (two), was accustomed know the severity of structural damage. For the excitation stress wave signal of the PPT actuator, a swept sine trend with a broad frequency range offered a positive excitation for checking functions since it contained low to high frequency result indicators [ten]. The excitation signals which were produced out of the performance generator were ten V (peak to peak) and also were amplified by the power amplifier of up to hundred V. The sampling frequency of the signals gotten by each PPT sensor channel was fifty kHz, obtained utilizing an NI-DAQ-6259 information acquisition system. For every specimen, when a specified drift ratio is covered under cyclic loading, the PPTs are used in order to do SHM and also to locate harm of the sample. Figure 4.4 shows the idea of local injury detection; the wall board is split into 3 areas (each region and path) has a primary actuator. The severities of harm in the real difference regions are compared and severe damage is situated. For starters, actuator A1, as depicted in Figures 4.1 along with 4.4, can be used to create an anxiety wave with frequencies of hundred Hz, one kHz as well as five kHz. Sensors S1 as well as S4, that are lodged in the wall sections as well as beams in a middling level, get the strain waves. The destruction index of Equation (two) is estimated as well as the harm express for every one of the propagation paths from A1 to S4, A3-S6 and A2-S5, is determined. Looking at the destruction indices which are gotten upon excitation by A1, A3 and A2 reveals the severity of harm for each road and also enables severe harm being situated. Inside SHM with a piezoelectric based sensing system, the plan of sensors and actuators might strongly affect the obtained values of the destruction index. Since the destruction status of a framework member between an actuator as well as sensor differs, now damage index is impacted by the locations of actuator and sensor. Thus, the proposed technique is a bit better suited to diagnosing neighborhood damage to a framework as in this particular examination than to diagnosing the general harm to the whole structure. For instance, in this particular study, actuator A2 was installed in the center of the foundation as well as sensor S2 was set up on the middle of the wall panel. The signal that was excited by A2 and also obtained by S2 could be utilized to identify the nearby damage status of the lower center of the wall panel. Though the sensitivity restrict in addition to resolution of the sensing product might be affected by the propagation distance of the excitation wave, the test results show the proposed injury list mirrors the severity of structural damage.



(a)



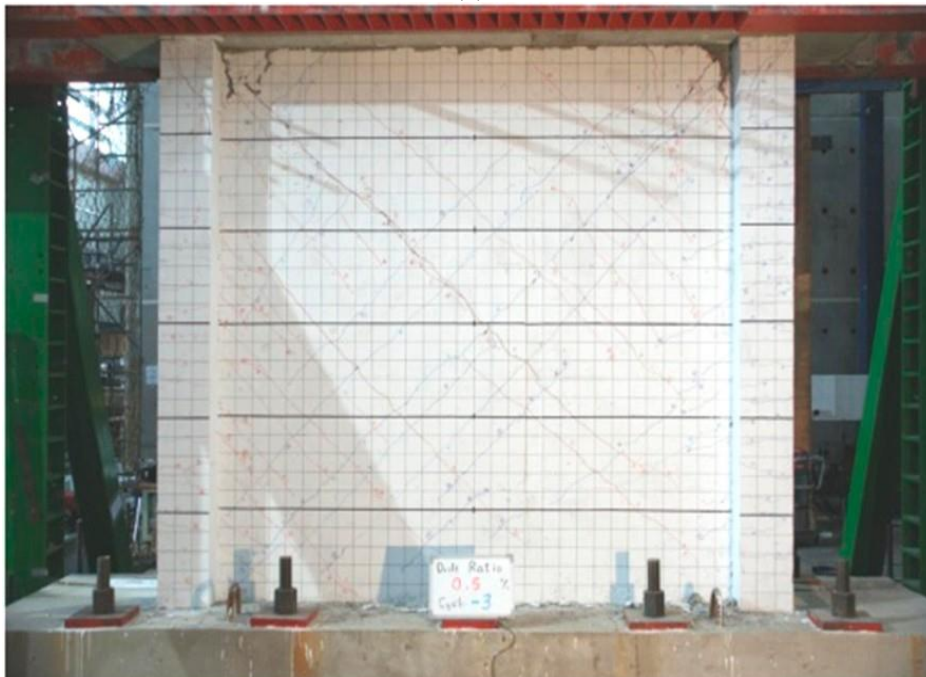
(d)

**Figure 4.2** Failure mode of the specimen RCW1 Cracking patterns of the specimen RCW1 at (a) drift 0.25%, (b) drift 0.5%, (c) drift 0.75% and (d) final failure mode at drift 1.0%.





(a)



(b)



(c)



(d)

**Figure 4.3**Cracking patterns of the specimen RCW2 at (a) drift 0.25%, (b) drift 0.5%, (c) drift 0.75% and (d) final failure mode at drift 1.0%.

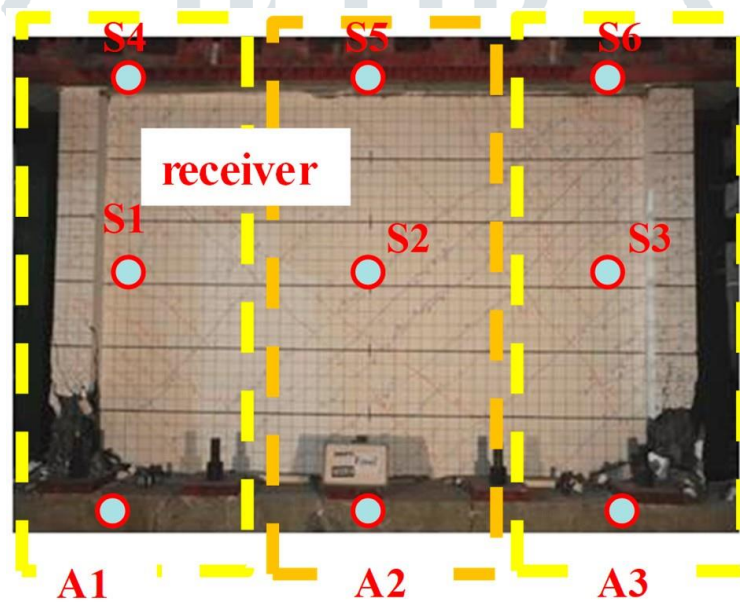


**Figure 4.4** 11Regions and sensor locations for damage detection

Since the results obtained from the excitation frequency of 5000 Hz is similar to 1000 Hz, the work only demonstrates the results obtained from the excitation frequencies of 100 Hz and 1000 Hz. Figures 4.5 and 4.6 show the damage indices of the sensors of RCW1 at various drift ratios under the various excitation frequencies of 100 Hz and 1000 Hz. According to these figures, the damage indices and damage state of each sensor in various frequencies have an increasing trend with the drift ratio increasing. In Figure 4.6, the damage indices of the sensors of S1, S4, S3 and S6 at the drift ratio of 1.0% are relatively higher than those of the sensors of S2 and S5. It can be observed that the damage state in the two sides of the wall is more serious than the center area. Additionally, the results have a high correlation with the final failure pattern of the specimen including the concrete crush in the bottom region of the boundary columns. However, the damage indices obtained from the excitation frequency of 100 Hz, as shown in Figure 4.5, can not identify the location with the serious damage. The experimental results have demonstrated the effectiveness of the proposed damage index that can be used to evaluate the damage state of an RC wall structure. Additionally, the piezoceramic transducers have the ability to identify the serious damage location using the excitation waves with high frequency.

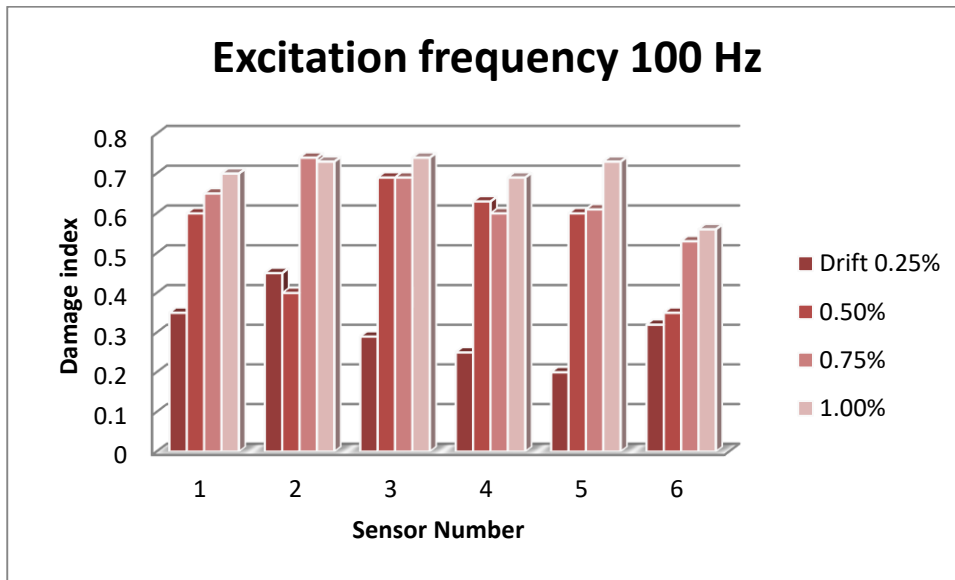


**Figure 4.4** Damage index at each drift ratio for RCW 1 (excitation frequency 100 Hz).

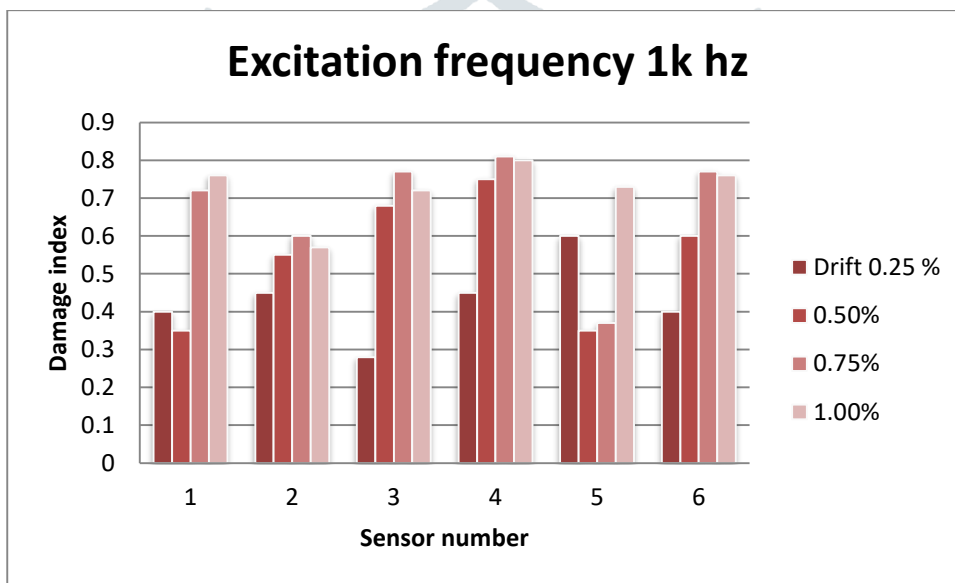


**Figure 4.5** Damage index at each drift ratio for RCW 1 (excitation frequency 1 kHz).

The loss of energy of a propagating stress wave that is caused by cracks or damage can be interestingly investigated in the frequency domain. For single-frequency excitation waves, the Fourier amplitude is concentrated around the designated excitation frequency in the frequency spectrum, so variation in the Fourier amplitude of received signals in the frequency spectrum can reveal the severity of damage in terms of the damage index that is defined in Equation(2). Figure 4.6 plots the time history of received sensor voltage and its corresponding Fourier amplitudes of sensor S4 under excitation by actuator A1 (frequency 5 kHz). The Fourier amplitudes around the frequency 5 kHz clearly decrease as the drift ratio of the specimen increases, indicating again the at the transmission energy of the stress waves is attenuated by cracks and damage.



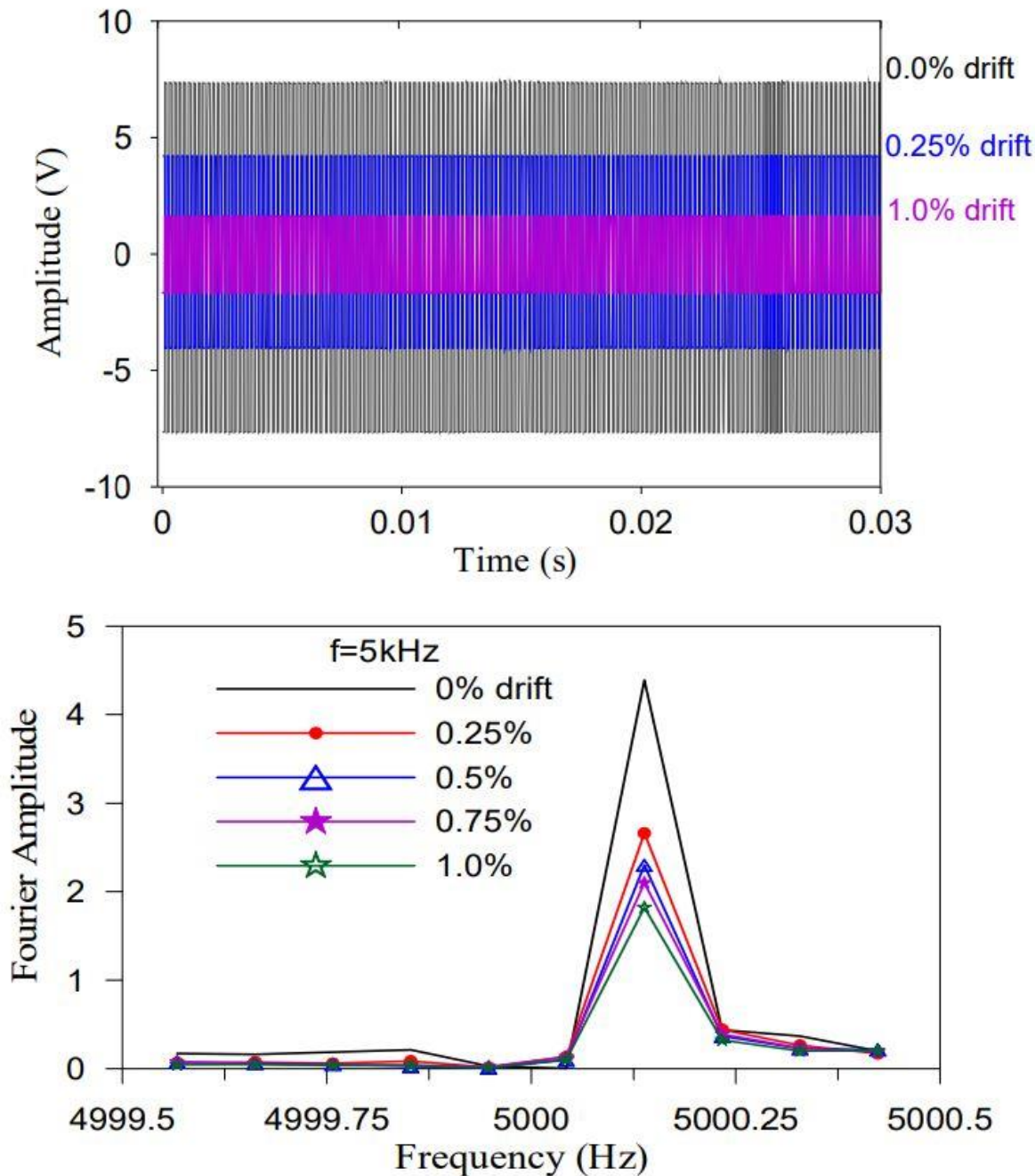


**Figure 4.6 (a)** Time history of received sensor voltage and **(b)** corresponding Fourier amplitude of sensor S4 for excitation frequency 5 kHz

Figures 4.7 and 4.8 plot the testing results of specimen RCW2 at various drift ratios under excitation frequencies of 100 Hz and 1000 Hz, respectively. As the drift ratio increases, the damage indices of each PZT sensor increase, revealing a trend similar to that in Figures 4.4 and 4.5. According to Figure 4.7, the damage indices of sensors S4-S6 at the final drift ratio of 1.0% are higher than those of sensors S1-S3, mainly because the damage state in the upper region of the wall is more serious than that in the bottom region. The results are also strongly correlated with the final failure pattern of the specimen, including concrete spalling in the top region of the wall panel and crushing of the concrete in the boundary columns. Minor interface cracks between the existing top beam and the wall panel are observed at a drift ratio of 0.25% during the test. The damage index of sensor S5 in Figure 4.7 is obviously higher than the indices of other sensors, especially sensor S2, at this drift ratio. This result is consistent with experimental observations and demonstrates that a PPS sensor can effectively detect interface cracks between structural members. Experimental results demonstrate that the piezoceramic-based method not only provides sensitive structural health monitoring but also is effective in the location of damage in concrete wall structures.

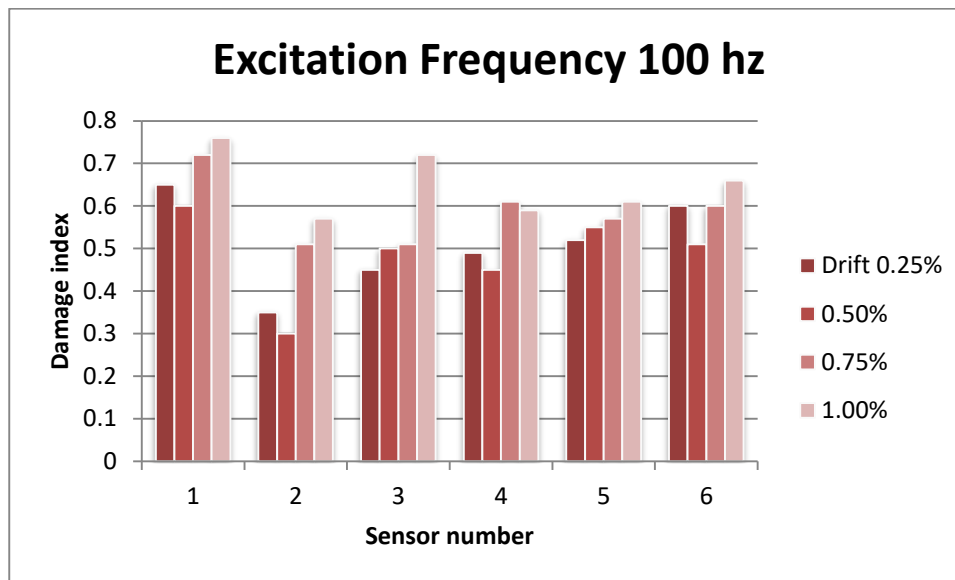


**Figure 4.7.**Damage index at each drift ratio for RCW2 (excitation frequency 100 Hz).

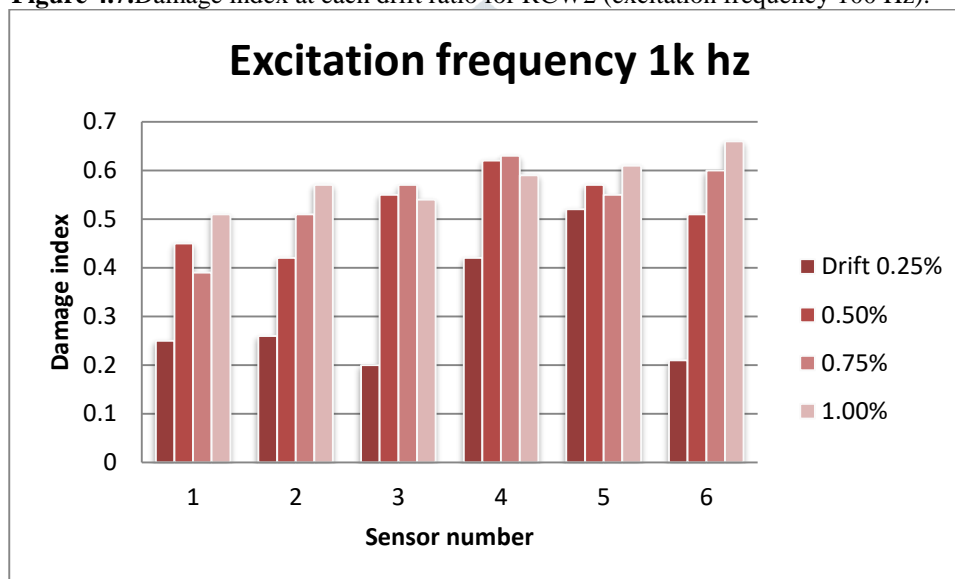


**Figure 4.8**Damage index at each drift ratio for RCW2 (excitation frequency 1 kHz)

## 5. CONCLUSION

In this particular work, two specimens with a post installed RC wall were evaluated under cyclic loading to analyze the SHM of these an RC wall underneath the seismic loading. A multi-functional transducer unit (post embedded PZT sensor) is utilized for Local damage detection and shm in this particular experimental test. The experimental results indicate the sensors were useful for the SHM of the entire structure and in identifying neighborhood damage of RC wall structures. With regard to retrofitted RC participants, the interface disaster or maybe cracks between 2 structural users (one current and one added) are essential and also influence the usefulness of the retrofit. Moreover, cracks or interface failure can't be noticed during renovation during retrofitting work. The experimental success in this effort show that PZT receptors could be utilized to recognize interface failure or maybe cracks between 2 structural users in retrofit building as well as assistance engineers to identify the degree of damage to a structure because after an earthquake. On account of the benefits of piezoelectric sensors, like their productive sensing, cost that is low, accessibility in several shapes, simplicity of ability and implementation to identify small splits from high frequency responses, piezoceramic based sensors have greater opportunity for any SHM detection of harm in RC wall structures compared to typical SHM methods. For comfort of implementation, potential labor must elucidate the connection between crack patterns, lengths or widths as well as the harm indices which are obtained by using PZT sensors

## REFERENCES

1. Brinda Chanv Prof. Sunil Bakhru & Prof. Vijay Mehta Structural health monitoring system using iot and Wireless technologies Dec 22-23, 2017
2. Debajyoti Misra Gautam Das Debaprasad Das an Iot Based Building Health Monitoring System Supported by Cloud, journal of Reliable Intelligent Environments 7 may 2020
3. Yang, Y., Hu, Y. and Lu, Y., "Sensitivity of PZT Impedance Sensors for Damage Detection of Concrete Structures", (2008).
4. Duan, W.H., Wang, Q. and Quek, S.T., "Applications of Piezoelectric Materials in Structural Health Monitoring and Repair: Selected Research Examples", (2010).

5. Yang, Y., Lim, Y.Y. and Soh, C.K.,” Practical issues related to the application of the electromechanical impedance technique in the structural health monitoring of civil structures: II. Numerical verification”, (2008), Smart Materials and Structures Volume 17 Number 3.
- 6.Zhang, Y., Xu, F., Chen, J., Wu, C. and Wen, D.,” Electromechanical Impedance Response of a Cracked Timoshenko Beam”, (2011).
- 7.Yang, Y. and Miao, A.,” Effect of External Vibration on PZT Impedance Signature”, (2008)
- 8.Chhabra, D., Narwal, K. and Singh, P.,” Design and Analysis of Piezoelectric Smart Beam for Active Vibration Control”, (2012).
- 9.Peng, D.,” Study on the Mechanical Characteristics of Steel Fiber Reinforced Concrete Crack using Strain Gauges for Structure Health Monitoring”, (2012).
10. Hong, K., Lee, J., Choi, S.W., Kim, Y. and Park, H.S.,” A Strain-Based Load Identification Model for Beams in Building Structures”, (2013).
- 11.Parameswaran, A.P., Pai, A.B., Tripathi, P.K. and Gangadharan, K.V.,” Active Vibration Control of a Smart Cantilever Beam on General Purpose Operating System”, (2013).
12. Hu, X., Zhu, H. and Wang, D.,” A Study of Concrete Slab Damage Detection Based on the Electromechanical Impedance Method”, (2014).
13. Neel Mania\*, Akhil Singh and Shastri L Nimmagadda An IoT Guided Healthcare Monitoring System for Managing RealTime Notifications by Fog Computing Services Procedia Computer Science 167 (2020) 850–859
14. Segun O. Olatinwo\* ,Trudi-H. Joubert Energy efficiency maximization in a wireless powered IoT sensor network for water quality monitoring 6 February 2020; Accepted 26 March 2020
- 15.OliverMörtha , Matthias Edera , Lukas IoT-based monitoring of environmental conditions to improve the production performance Procedia Manufacturing 45 (2020) 283–288
- 16.DonatoAbruzzese, Andrea Micheletti\*, Alessandro IoT sensors for modern structural health monitoring. A new frontier Procedia Structural Integrity 25 (2020) 378–385
- 17.Michal Dziendzikowski \*, PatrykNiedbala, ArturKurnyta, KamilKowalczyk and Krzysztof Dragan Structural Health Monitoring of a Composite Panel Based on PZT Sensors and a Transfer Impedance Framework Air Force Institute of Technology, ul. Ks. Bolesława 6, 01-494 Warszawa, Poland; patryk.niedbala@itwl.pl (P.N
- 18.Qiu Lei, Yuan Shenfang\*, Wang Qiang, Sun Yajie, Yang Weiwei ,Design and Experiment of PZT Network-based Structural Health Monitoring Scanning System ,Chinese Journal of Aeronautics 22(2009) 505-512
- 19.Hongduo Zhao , Luyao Qin , Jianming Ling ,Synergistic performance of piezoelectric transducers and asphalt pavement H. Zhao et al. / International Journal of Pavement Research and Technology 11 (2018) 381–387
- 20.ChristianFalconi ,Piezoelectric nanotransducers Nano Energy 59 (2019) 730–744
- 21.Debajyoti Misra1 · Gautam Das2 · DebaprasadDas,AnIoT based building health monitoring system supported by cloud Journal of Reliable Intelligent Environments
- 22.Bhawani Shankar Chowdhry1 · Ali Akbar Shah Development of IOT Based Smart Instrumentation for the Real Time Structural Health Monitoring Wireless Personal Communications <https://doi.org/10.1007/s11277-020-07311-4>

